Journal of Molecular Liquids 188 (2013) 196–202

Contents lists available at ScienceDirect

Journal of Molecular Liquids

journal homepage: www.elsevier.com/locate/molliq

Thermophysical properties of $[C_{N-1}C_1im][PF_6]$ ionic liquids

Marisa A.A. Rocha [a,*], Filipe M.S. Ribeiro [a], Ana I.M.C. Lobo Ferreira [a], João A.P. Coutinho [b], Luís M.N.B.F. Santos [a,*]

[a] CIQ, Departamento de Química e Bioquímica, Faculdade de Ciências da Universidade do Porto, R. Campo Alegre 687, P-4169-007, Porto, Portugal
[b] CICECO, Departamento de Química, Universidade de Aveiro, P-3810-193 Aveiro, Portugal

ARTICLE INFO

Article history:
Received 25 June 2013
Received in revised form 30 August 2013
Accepted 9 September 2013
Available online 18 October 2013

Keywords:
Refractive indices
Viscosities
Densities
Hexafluorophosphate
Nanostructuration
Ionic liquids
Trend shift
Imidazolium
Alkyl chain effect

ABSTRACT

Densities, viscosities and refractive index, as a function of temperature, and isobaric thermal expansion coefficient, were determined for 1-alkyl-3-methylimidazolium hexafluorophosphate, $[C_{N-1}C_1im][PF_6]$ (where N = 5 to 10) series of ionic liquids. The density presents a regular decrease along the ionic liquid series, with no detectable alkyl chain length dependence of the thermal expansion coefficient. Both the refractive index and viscosity show a trend shift along the series around the $[C_6C_1im][PF_6]$ that could be associated to the impact of the change in the nanostructuration of the ionic liquids. The experimental results are compared with the analogous $[C_{N-1}C_1im][NTf_2]$ series and the effect of the anion is analyzed. The sphericity of the $[PF_6]^-$ anion is reflected in the lower pre-exponential VTF parameter, A_η, and the higher viscosity of the $[C_{N-1}C_1im][PF_6]$, when compared with the $[C_{N-1}C_1im][NTf_2]$ series, is ruled by the higher energy barriers, which are related with stronger electrostatic interaction due to the low charge dispersion of the $[PF_6]^-$.anion.

1. Introduction

The physicochemical properties of ionic liquids can vary considerably depending on the combination of cations and anions. Therefore, for the interpretation of their properties and a successful modeling of ionic liquids, highly accurate data regarding these physicochemical properties are needed, such as heat capacities, vapor pressures, viscosities, densities and refraction index. Recently, we reported several thermodynamic studies of the extended series of ILs $[C_{N-1}C_1im][NTf_2]$ (with N = 3–9, 11, and 13), and of the symmetric $[C_{N/2}C_{N/2}im][NTf_2]$ (with N = 4–24) [1–4]. Based on these works, it was possible to highlight the effect of the nanostructuration of $[C_{N-1}C_1im][NTf_2]$ and $[C_{N/2}C_{N/2}im][NTf_2]$ ionic liquid series and to evaluate the effect of the cation topological symmetry on the thermodynamic properties of vaporization, heat capacities and viscosity data. Understanding the impact of nanostructuration on the thermophysical properties of ionic liquids is highly relevant but previous works used only the even numbered ionic liquids, and consequently the complete characterization of important trends which are related with the nanostructuration is not possible, neither the identification of the outlier character of $[C_1C_1im][NTf_2]$ and $[C_2C_1im][NTf_2]$ [1–4].

In this work, the thermophysical properties of 1-alkyl-3-methylimidazolium hexafluorophosphate, $[C_{N-1}C_1im][PF_6]$ (with N = 5–10), specifically density, viscosity and refractive index, and their dependency with temperature were measured. Concerning this family of ionic liquids, most of the thermophysical studies have been focused on the following liquids: $[C_4C_1im][PF_6]$, $[C_6C_1im][PF_6]$ and $[C_8C_1im][PF_6]$, which prevent the identification of the nanostructuration on these ionic liquids [5–31]. The experimental results obtained will be used to evaluate the effect of the chemical nature of the anion, sphericity, and size, as well as the overall impact of the nanostructuration on the thermophysical properties of these ionic liquids.

2. Experimental section

2.1. Materials and purification

The 1-alkyl-3-methylimidazolium hexafluorophosphate, $[C_{N-1}C_1im][PF_6]$ (with N = 5–10), used in this work, was purchased from IOLITEC with a stated purity of better than 99%. All the ionic liquids were dried and purified under vacuum (<10 Pa) at moderate temperature (323 K) and constant stirring, in order to reduce the

* Corresponding authors. Tel.: +351 220402836; fax: +351 220402659.
E-mail addresses: marisa.alexandra.rocha@gmail.com (M.A.A. Rocha), lbsantos@fc.up.pt (L.M.N.B.F. Santos).

0167-7322/$ – see front matter © 2013 Elsevier B.V. All rights reserved.
http://dx.doi.org/10.1016/j.molliq.2013.09.031

Table 1
Experimental results of density, ρ, at 0.1 MPa for the $[C_{N-1}C_1im][PF_6]$ ionic liquid series as a function of temperature.

T/K	ρ/(kg·m^{-3})					
	$[C_4C_1im][PF_6]$	$[C_5C_1im][PF_6]$	$[C_6C_1im][PF_6]$	$[C_7C_1im][PF_6]$	$[C_8C_1im][PF_6]$	$[C_9C_1im][PF_6]$
293.15	1371.8	1332.2	1298.5	1266.7	1240.9	1217.0
298.15	1367.4	1327.8	1294.2	1262.6	1236.9	1213.1
303.15	1363.2	1323.7	1290.1	1258.5	1232.9	1209.2
308.15	1359.0	1319.6	1286.1	1254.5	1229.0	1205.3
313.15	1354.9	1315.5	1282.1	1250.6	1225.1	1201.5
318.15	1350.8	1311.6	1278.2	1246.8	1221.3	1197.8
323.15	1346.8	1307.6	1274.3	1243.0	1217.6	1194.1
328.15	1342.7	1303.7	1270.5	1239.3	1213.9	1190.4
333.15	1338.7	1299.8	1266.7	1235.5	1210.2	1186.8
338.15	1334.7	1295.9	1262.9	1231.8	1206.6	1183.2
343.15	1330.6	1292.0	1259.1	1228.1	1202.9	1179.6
348.15	1326.6	1288.1	1255.3	1224.4	1199.3	1176.0
353.15	1322.7	1284.3	1251.5	1220.7	1195.6	1172.4
358.15	1318.7	1280.4	1247.7	1217.0	1192.0	1168.8
363.15	1314.8	1276.6	1244.0	1213.3	1188.4	1165.3

Note: the magnitude of the experimental differentiation between the two independent set of density data: ± 0.2 kg·m^{-3}.

presence of water or other volatile contents. This process was performed systematically before and during the thermophysical property measurements.

2.2. Density and viscosity

The density, ρ, and dynamic viscosity, η, measurements were performed with an automated SVM 3000 Anton Paar rotational Stabinger viscometer–densimeter. The description concerning the operation of this equipment is available in the literature [32]. The measurements were carried out at atmospheric pressure in the temperature range from 293.15 to 363.15 K for the pure ionic liquids. The apparatus was calibrated using the three standard calibration samples, APN7.5, APN26 and APN415 in the same experimental conditions of the ionic liquid measurements. The reproducibility of the dynamic viscosity and density measurements is, according to the manufacturer, 0.35% and $\pm$ 0.5 kg·m^{-3}, respectively from 288.15 K to 378.15 K and the uncertainty of temperature is within ± 0.02 K. For each ionic liquid, at least two independent measurements of the density and viscosity were performed, using the same experimental conditions and different samples.

2.3. Refractive index

The refractive indices were measured at the sodium D-line using a Bellingham model RFM340 refractometer ($\pm 3 \times 10^{-5}$ stated precision), as a function of temperature (288.15 to 318.15) K. The apparatus was calibrated with degassed water (Millipore quality) and toluene (Spectranal, 99.9%). The temperature in the refractometer cell is controlled using an external thermostatic bath within a temperature fluctuation of ($\pm 5 \times 10^{-3}$) K, measured with a resolution better than 1×10^{-3} K and an uncertainty within ± 0.02 K. Samples were directly introduced into the flow cell (prism assembly) using a syringe; the flow cell was kept closed after sample injection. For each ionic liquid at least two independent experiment were performed and in each experiment at least three measurements were taken at each temperature. The refractive indices were measured with respect to air and no corrections were applied.

3. Results and discussion

3.1. Density

The experimental density data for the studied ionic liquids are presented in Table 1. Fig. 1 displays the logarithm of density as a function of temperature and the respective relative deviations between the experimental density measured in this work and those reported in the literature.

The experimental density data, in the temperature range, was described using a second order polynomial equation correlation, according to Eq. (1):

$$\ln(\rho/\mathrm{kg}\cdot\mathrm{m}^{-3}) = a + b\cdot T + c\cdot T^2 \quad (1)$$

The comparison with the literature data was limited due to the lack of data for the odd number of the studied ionic liquids series ($[C_5C_1im][PF_6]$, $[C_7C_1im][PF_6]$ $[C_9C_1im][PF_6]$). Only densities of three ionic liquids, $[C_4C_1im][PF_6]$, $[C_6C_1im][PF_6]$ and $[C_8C_1im][PF_6]$, were found in the literature. The densities obtained in this work are in good agreement with the literature results, with deviations under 0.1% [12,33]. Higher

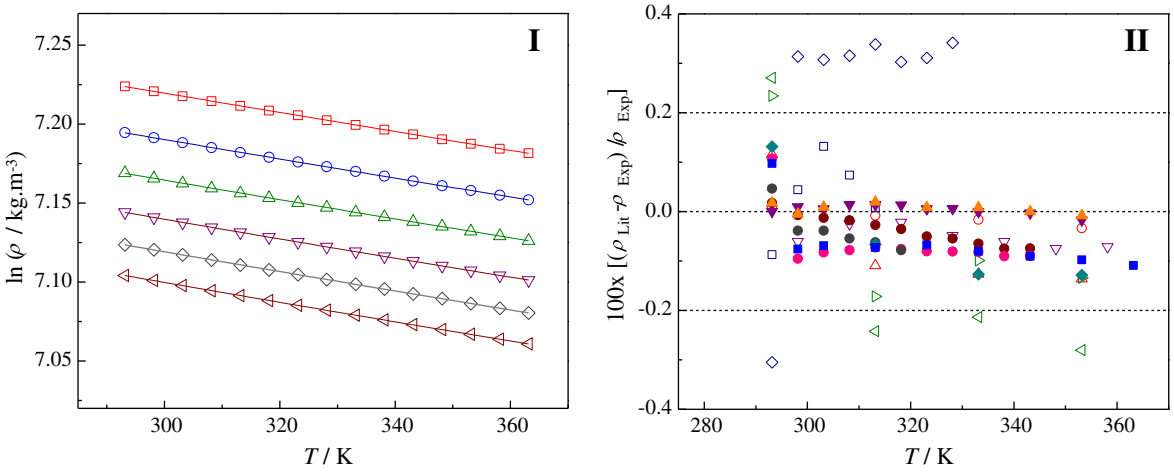

Fig. 1. (I) Logarithm of density as a function of temperature for $[C_{N-1}C_1im][PF_6]$ ionic liquid family. The thin lines results from the linear fitting of the experimental results. □ – $[C_4C_1im][PF_6]$; ○ – $[C_5C_1im][PF_6]$; △ – $[C_6C_1im][PF_6]$; ▽ – $[C_7C_1im][PF_6]$; ◇ – $[C_8C_1im][PF_6]$; ◁ – $[C_9C_1im][PF_6]$.(II) Relative deviations between the experimental density measured in this work (ρ_{exp}) and those reported in the literature (ρ_{exp}) as a function of temperature for $[C_{N-1}C_1im][PF_6]$ ionic liquid series. Tomida et al. [13] ◆ – $[C_4C_1im][PF_6]$; Y. Geng et al. [14] ◇ – $[C_4C_1im][PF_6]$; D. Tomida et al. [15] ◁ – $[C_6C_1im][PF_6]$, ▷ – $[C_8C_1im][PF_6]$; Taguchi et al. [16] △ – $[C_6C_1im][PF_6]$, ○ – $[C_8C_1im][PF_6]$; A.B. Pereiro et al. [20] ● – $[C_4C_1im][PF_6]$, ● – $[C_8C_1im][PF_6]$; W. Fan et al. [21] ▼ – $[C_4C_1im][PF_6]$; K. R. Harris et al. [22] ▲ – $[C_8C_1im][PF_6]$; K. R. Harris et al. [23] ■ – $[C_6C_1im][PF_6]$; Tokuda et al. [25] □ – $[C_4C_1im][PF_6]$; A. Muhammad et al. [26] ▽ – $[C_6C_1im][PF_6]$; A.B. Pereiro et al. [31] ● – $[C_6C_1im][PF_6]$.

Table 2
Fitting parameters of the equation, $\ln(\rho/\mathrm{kg}\cdot\mathrm{m}^{-3}) = a + b.T + c.T^2$, density, molar volume and the thermal expansion coefficients, α_p, at 323.15 K and 0.1 MPa for the studied ionic liquids.

Ionic liquid	a	$10^4 \times b$ / K^{-1}	$10^7 \times c$ / K^{-2}	ρ (T = 323.15 K) / (kg·m^{-3})	V_m (T = 323.15 K) / (cm^3·mol^{-1})	$10^3 \times \alpha_p$(T = 323.15 K) / K^{-1}
[C_4C_1im][PF_6]	7.4175 ± 0.0035	−7.07 ± 0.21	1.56 ± 0.33	1346.8	211.0	0.606 ± 0.030
[C_5C_1im][PF_6]	7.3974 ± 0.0048	−7.62 ± 0.29	2.38 ± 0.44	1307.6	228.1	0.608 ± 0.041
[C_6C_1im][PF_6]	7.3765 ± 0.0055	−7.89 ± 0.34	2.74 ± 0.51	1274.3	245.0	0.612 ± 0.047
[C_7C_1im][PF_6]	7.3562 ± 0.0058	−8.14 ± 0.36	3.08 ± 0.54	1243.0	262.5	0.615 ± 0.050
[C_8C_1im][PF_6]	7.3381 ± 0.0049	−8.27 ± 0.30	3.22 ± 0.45	1217.6	279.5	0.619 ± 0.042
[C_9C_1im][PF_6]	7.3175 ± 0.0039	−8.17 ± 0.24	3.02 ± 0.36	1194.1	296.7	0.622 ± 0.033

relative deviations on density, in the range between −0.32% and 0.25% for [C_4C_1im][PF_6] [13–34], [C_6C_1im][PF_6] [14,15], and [C_8C_1im][PF_6] [14] were observed, which in these cases could be attributed to the low quality of the ionic liquid samples (namely water and halide content) [12–17,32,34–41].

From the parameters obtained from the fitting of the density data using Eq. (1), the temperature dependence of the isobaric thermal expansion coefficients (α_p) were derived, using the following equation:

$$\alpha_p = -\frac{1}{\rho}\left(\frac{\partial\rho}{\partial T}\right)_p = -\left(\frac{\partial \ln\rho}{\partial T}\right)_p = -(b + 2c\cdot(T/\mathrm{K})) \quad (2)$$

where, ρ is the density in kg·m^{-3}, T is the temperature in K, p is the pressure, and b and c represent the parameters of Eq. (1). The fitting parameters of Eq. (1) and the thermal expansion coefficients, at 323.15 K and 0.1 MPa, for all the studied ionic liquids are listed in Table 2. The graphic representations of the molar volumes and thermal expansion coefficients, at 323.15 K (data is presented at T = 323.15 K, in order to compare with the data available in the literature for the [$C_{N-1}C_1$im][NTf_2] series [4,42] and for [C_3C_1im][PF_6]. [43]) and 0.1 MPa, against the total number of carbons of the alkyl side chains length, N, are presented in Fig. 2.

It can be observed that the derived molar volume increment at (323.15 K) for each $-CH_2-$ is identical for both IL series ([PF6]$^-$, [NTf_2]$^-$) and very close to the typical value for alkanes [45]. For the same number of carbons in the alkyl chain, N, the hexafluorophosphate based ionic liquids presents lower density and lower thermal expansion coefficients when compared with the [$C_{N-1}C_1$im][NTf_2] IL series [4,42]. Considering the associated uncertainty, the thermal expansion coefficients are constant with the alkyl side chain of the cation. The lower thermal expansion coefficients observed for the IL with the [PF_6]$^-$ anion when compared with the [NTf_2]$^-$ should be related with the higher conformational flexibility of the [NTf_2]$^-$ anion. The increase of the molar volume arising from the [PF_6]$^-$ anion is due only to the increase of the translation dynamics of the spherical anion and the small increase of the occupied vibrational mode. In the case of the [NTf_2]$^-$ anion, the higher increase of the molar volume with the temperature and consequently higher thermal expansion coefficient is related with the high flexibility and several possible configurationally conformers of the bistriflamide anion, and additionally several internal rotors will also contribute. Fig. 1(II) depicts the predicted thermal expansion coefficients by the Gardas and Coutinho [44] group contribution method for comparison.

3.2. Viscosity

The experimental viscosity data for the studied ionic liquids are reported in Table 3. Fig. 3 depicts the graphic representations of the $\ln(\eta/\mathrm{mPa\cdot s})$ against the temperature and the deviations between the experimental viscosity measured in this work and those reported in the literature, respectively.

The data presented in this work show a good agreement with several literature data sources, as shown in Fig. 3(II) [12,13,15,19–23]. The data reported by Branco et al. [24] for [C_4C_1im][PF_6] and [C_8C_1im][PF_6] and by Geng et al. [14] for [C_4C_1im][PF_6], present a large negative deviation between 22% and 50% from our results, which could be related with the higher water content, which leads to a significant decrease of the viscosity [14,24,25]. The data published previously by Huddleston et al. [8], presents a positive deviations of 40% for [C_4C_1im][PF_6] and 17% for [C_6C_1im][PF_6] from our data. The positive deviation for these ionic liquids is usually related with the higher chloride impurities, which lead to a significant increase of the viscosity [8,12,17,26]. The effect of water content and chloride impurities on the viscosity and density of ionic liquids has been already evaluated in the literature, and was shown that the presence of very low concentrations of chloride

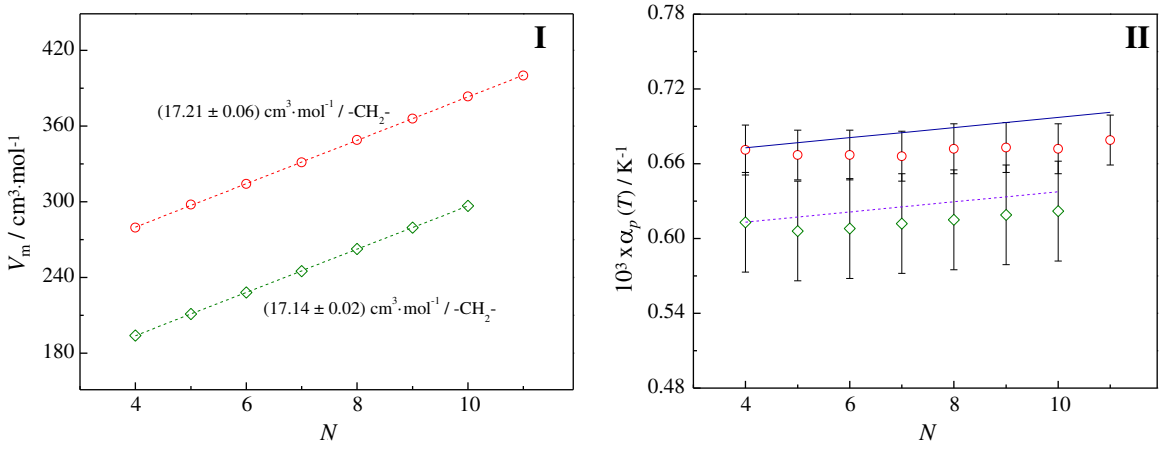

Fig. 2. Graphical representation of the (I) molar volumes and (II) thermal expansion coefficient, at 323.15 K and 0.1 MPa, as a function of the total number of carbons of the alkyl side chains length, N. ○ – [$C_{N-1}C_1$im][NTf_2] (with N = 4–11) [4].; ◇ - [C_3C_1im][PF_6] [29]; [$C_{N-1}C_1$im][PF_6] (with N = 5–10). Gardas and Coutinho group contribution [44], values calculated at 298.15 K: – – – – [$C_{N-1}C_1$im][PF_6] (N = 4–10) and – – [$C_{N-1}C_1$im][NTf_2] (with N = 4–11).

Table 3
Experimental viscosity results, η, at 0.1 MPa for the $[C_{N-1}C_1im][PF_6]$ ionic liquid series as a function of temperature.

T/K	η/(mPa·s)					
	[C_4C_1im][PF_6]	[C_5C_1im][PF_6]	[C_6C_1im][PF_6]	[C_7C_1im][PF_6]	[C_8C_1im][PF_6]	[C_9C_1im][PF_6]
293.15	373.95	537.91	694.11	821.98	1044.8	1319.90
298.15	269.03	380.06	482.86	568.36	711.88	892.92
303.15	200.02	277.57	347.71	407.03	503.46	624.37
308.15	151.96	207.41	256.98	298.44	364.84	447.45
313.15	118.20	158.86	194.75	224.76	271.98	330.25
318.15	92.709	122.70	148.68	170.48	204.31	245.78
323.15	74.230	96.844	116.11	132.43	157.08	187.13
328.15	60.266	77.608	92.133	104.44	122.76	144.94
333.15	49.717	63.228	74.355	83.812	97.641	114.29
338.15	41.372	51.907	60.514	67.831	78.386	91.025
343.15	34.872	43.210	49.976	55.725	63.89	73.660
348.15	29.678	36.347	41.732	46.321	52.664	60.366
353.15	25.550	30.932	35.255	38.946	43.974	49.986
358.15	22.074	26.469	29.987	32.984	37.024	41.848
363.15	19.261	22.878	25.769	28.220	31.489	35.378

Note: the magnitude of the experimental differentiation between the two independent set of viscosity data: ±[0.005 mPa·s + 0.001.(η/mPa·s)].

Table 4
Fitting coefficients of VFT equation for the viscosity data of the studied ionic liquids and the derived energy barrier at 323.15 K.

Ionic Liquid	A_η/(mPa.s)	B_η/K	C_η/K	$E(T = 323.15\ K)$/(kJ·mol^{-1})
[C_4C_1im][PF_6]	0.133 ± 0.004	934 ± 8	175.6 ± 0.7	37.2 ± 0.8
[C_5C_1im][PF_6]	0.100 ± 0.003	1036 ± 9	172.6 ± 0.6	39.7 ± 0.8
[C_6C_1im][PF_6]	0.088 ± 0.003	1084. ± 11	172.3 ± 0.8	41.4 ± 1.0
[C_7C_1im][PF_6]	0.077 ± 0.003	1137 ± 11	170.6 ± 0.8	42.4 ± 1.0
[C_8C_1im][PF_6]	0.066 ± 0.003	1192 ± 13	169.9 ± 0.8	44.1 ± 1.1
[C_9C_1im][PF_6]	0.055 ± 0.002	1260 ± 13	168.2 ± 0.8	45.6 ± 1.1

in the ionic liquid sample drastically increases the viscosity, whereas the presence of water reduces the viscosity [12,17,46,47].

Various theoretical models and empirical or semi-empirical expressions are available in the literature to correlate the viscosity of liquids as a function of pressure and temperature [48]. In this work, the Vogel–Tammann–Fulcher equation (VTF) [48–51] was used to correlate the experimental viscosity data:

$$\ln(\eta/\mathrm{mPa}\cdot\mathrm{s}) = \ln\left(A_\eta/\mathrm{mPa}\cdot\mathrm{s}\right) + \frac{B_\eta}{\left(T - C_\eta\right)} \tag{3}$$

where η is the viscosity in mPa·s, T is the temperature in K, and A_η, B_η and C_η are the adjustable parameters. The parameters were determined from the fitting of the experimental data using the Eq. (3) for the studied ionic liquids. The parameters of VTF equation are presented in Table 4. The correlated viscosities, represented as the solid lines in Fig. 3(I), are in good agreement with the experimental data.

The energy barrier of the fluid to a shear stress, E, can be evaluated based in the viscosity dependence with the temperature using the following equation:

$$E = R\cdot\frac{\partial(\ln\eta)}{\partial(1/T)} = R\cdot\left(\frac{B_\eta}{\left(\frac{C_\eta^2}{T^2} - \frac{2\cdot C_\eta}{T} + 1\right)}\right). \tag{4}$$

In this work, the energy barrier, E, was derived at $T = 323.15$ K in order to compare with the literature data for $[C_{N-1}C_1im][NTf_2]$ and evaluate the effect of the anion [4,52]. The plots of viscosity at $T = 323.15$ K as a function of the total number of carbon atoms in the alkyl chains in the cation, for the $[C_{N-1}C_1im][PF_6]$ and their comparison with the $[C_{N-1}C_1im][NTf_2]$, are depicted in Fig. 4. The literature values obtained for the $[C_3C_1im][PF_6]$ for the discussion was considered [43]. The pre-exponential coefficient of the VTF equation, A_η, and the energy barrier at $T = 323.15$ K as a function of the total number of carbon atoms in the alkyl chains of the cation, are presented in Fig. 5. The predicted parameters, A_η and energy barriers from the Gardas and Coutinho [44] group contribution method (plotted in Fig. 5) are in quite reasonable agreement with the experimental results.

Unlike the dependency of the density with the alkyl side chain length previously observed, there is an increase of the viscosity along the studied ionic liquid series as shown in Fig. 4. A shift in the viscosities

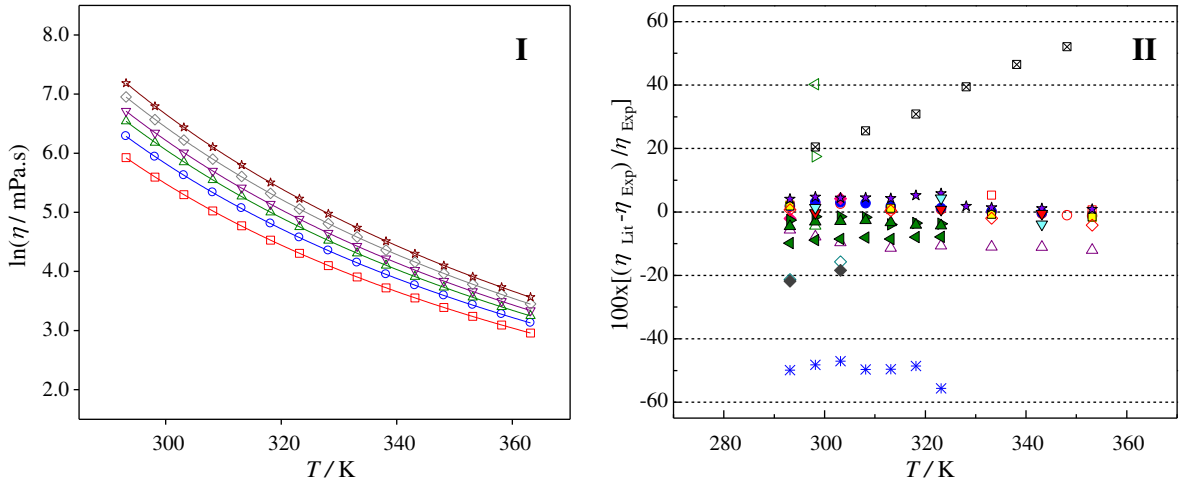

Fig. 3. (I) Graphic representation of $\ln(\eta/\mathrm{mPa}\cdot\mathrm{s}) = f(T)$ for for$[C_{N-1}C_1im][PF_6]$ ionic liquid family. The solid lines represent the Vogel–Tammann–Fulcher fittings (Eq. (3)). □ – [C_4C_1im][PF_6]; ○ – [C_5C_1im][PF_6]; △ – [C_6C_1im][PF_6]; ▽ – [C_7C_1im][PF_6]; ◇ – [C_8C_1im][PF_6]; ⋆ – [C_9C_1im][PF_6]. (II) Relative deviations between the experimental density measured in this work (ρ_{exp}) and those reported in the literature (ρ_{exp}) as a function of temperature for $[C_{N-1}C_1im][PF_6]$ ionic liquid series. J. G. Huddleston et al. [8] ▷ – [C_4C_1im][PF_6], ◁ – [C_6C_1im][PF_6], △ – [C_8C_1im][PF_6]; D. Tomida et al. [13] □ – [C_4C_1im][PF_6]; Y. Geng et al. [14] ⁎ – [C_4C_1im][PF_6]; D. Tomida et al. [15] ■ – [C_6C_1im][PF_6]; A. Ahosseini et al. [19] ▼ – [C_6C_1im][PF_6] (Oscillating-piston viscosimeter), ▼ – [C_6C_1im][PF_6] (Cone-and-plate viscosimeter); A. B. Pereiro et al. [20] ◀ – [C_4C_1im][PF_6], ▶ – [C_6C_1im][PF_6], ▲ – [C_8C_1im][PF_6]; ◇ – [C_8C_1im][PF_6]; W. Fan et al. [21] ★ – [C_4C_1im][PF_6]; K. R. Harris et al. [22] ● – [C_8C_1im][PF_6]; K. R. Harris et al. [23] ○ – [C_6C_1im][PF_6]; L. C. Branco et al. [24] ◇ – [C_4C_1im][PF_6], ◆ – [C_6C_1im][PF_6], ◆ – [C_8C_1im][PF_6]; H. Tokuda et al. [25] △ – [C_4C_1im][PF_6]; A. Muhammad et al. [26] ⊠ – [C_6C_1im][PF_6].

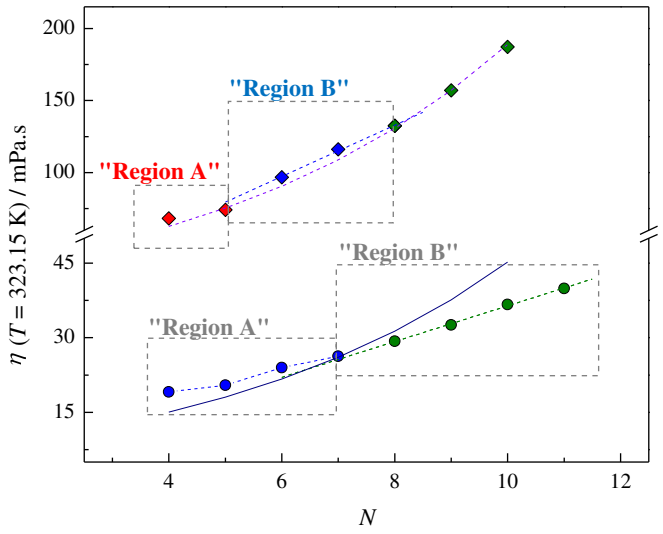

Fig. 4. Plots of viscosity (η/mPa··s) at $T = 323.15$ K and 0.1 MPa for the $[C_{N-1}C_1im][PF_6]$ and the Comparison of the viscosity (η/mPa·s) at $T = 323.15$ K and 0.1 MPa. ♦ — $[C_3C_1im][PF_6]$ [43]; $[C_{N-1}C_1im][PF_6]$ (with $N = 5$–10); ● — $[C_{N-1}C_1im][NTf_2]$ (with $N = 4$–11) [4,51]. Gardas and Coutinho group contribution [44]: – – – — $[C_{N-1}C_1im][PF_6]$ ($N = 4$–10) and – – $[C_{N-1}C_1im][NTf_2]$ (with $N = 4$–10).

along the $[C_{N-1}C_1im][PF_6]$ ILs series starting at $[C_5C_1im][PF_6]$, similar to that previously identified in the bistriflamide, $[C_{N-1}C_1im][NTf_2]$, series, was here observed [4]. This trend shift is related with the structural organization of the liquid above a Critical Alkyl Length Size, (CALS). Due to the bulkier, $[NTf_2]^-$ anion the CALS for $[PF_6]^-$ is shifted to shorter alkyl side chains. This is in good agreement with MD results showing that the CALS for $[PF_6]$-based ILs [53] takes place at shorter chain lengths than for $[NTf_2]$-based ILs [1].

In "Region A" ($[C_3C_1im][PF_6]$ and $[C_4C_1im][PF_6]$), the increase on the viscosity, is smaller than the observed in "Region B" ($[C_5C_1im][PF_6]$ and $[C_7C_1im][PF_6]$) which presents a linear and more pronounced increase on the viscosity. Starting from $[C_7C_1im][PF_6]$, the viscosity shows a progressive positive deviation (higher viscosities) from the linear behavior in "Region B". The ionic liquids with the $[PF_6]^-$ anion present significantly higher viscosities than the bistriflamide based ILs and the higher contribution of the $[PF_6]^-$ anion to the viscosity increases with the alkyl side chain length. In Fig. 5(I), two regions in the pre-exponential parameter of the VTF equation, A_η, could be identified. Starting from $[C_5C_1im][PF_6]$ until $[C_9C_1im][PF_6]$, a linear decrease of the pre-exponential parameter, similar to that present in the $[C_{N-1}C_1im][NTf_2]$ series, is observed [4]. Additionally $[C_{N-1}C_1im][PF_6]$ ILs present lower A_η comparing with the $[C_{N-1}C_1im][NTf_2]$ series, that is related with the sphericity of the $[PF_6]^-$ anion.

The energy barrier at 323.15 K, E, (Fig. 5(II)), for the $[C_{N-1}C_1im][PF_6]$ series increases monotonously in both regions and is ~10 kJ·mol^{-1} higher than in the $[NTf_2]$ ILs. The contribution per methylene group for the energy barriers for the $[C_{N-1}C_1im][PF_6]$ seems to be slightly higher than for the $[C_{N-1}C_1im][NTf_2]$ (1.5 kJ·mol^{-1}, against 1.0 kJ·mol^{-1} per $-CH_2-$) [4]. The shorter members $[C_3C_1im][PF_6]$ and $[C_4C_1im][PF_6]$ have identical and lower energy barrier, E, than would be expected from the extrapolation of the homolog series trend. This could be related with a balance between the decrease in the electrostatic interactions and the increase in the intermolecular interactions arising from the increase of the alkyl side length. The higher viscosity of the $[C_{N-1}C_1im][PF_6]$ when compared with the $[C_{N-1}C_1im][NTf_2]$ series is ruled by the higher energy barriers, which are related with their higher intermolecular interactions and could be understood considering the low charge dispersion of the

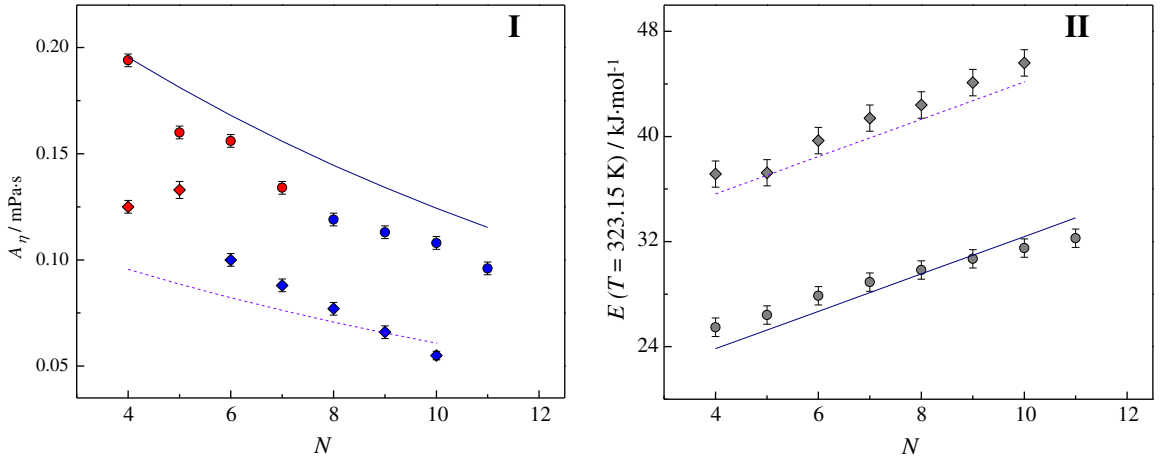

Fig. 5. Graphical representation of the pre-exponential coefficient of the Vogel–Tammann–Fulcher equation (A_η/mPa·s) (I), energy barrier (E/kJ·mol^{-1}) at $T = 323.15$ K (II) as function of the total number of carbon atoms in the alkyl side chains of the cation, N, for ♦ — $[C_3C_1im][PF_6]$ [43], $[C_{N-1}C_1im][PF_6]$ (with $N = 5$–10), this work; ● — $[C_{N-1}C_1im][NTf_2]$ (with $N = 4$–11) [4]. Gardas and Coutinho group contribution [44]: – – – — $[C_{N-1}C_1im][PF_6]$ ($N = 4$–10) and – – $[C_{N-1}C_1im][NTf_2]$ (with $N = 4$–11).

Table 5
Experimental refractive indices at the sodium D-line, n_D, at 0.1 MPa, for the studied ionic liquids as a function of temperature.

T/K	n_D					
	$[C_4C_1im][PF_6]$	$[C_5C_1im][PF_6]$	$[C_6C_1im][PF_6]$	$[C_7C_1im][PF_6]$	$[C_8C_1im][PF_6]$	$[C_9C_1im][PF_6]$
288.15	1.41211	1.41657	1.41980	1.42311	1.42576	1.42823
293.15	1.41078	1.41522	1.41844	1.42172	1.42434	1.42681
298.15	1.40945	1.41387	1.41708	1.42033	1.42293	1.42538
303.15	1.40812	1.41252	1.41572	1.41894	1.42152	1.42396
308.15	1.40679	1.41117	1.41436	1.41755	1.42011	1.42253
313.15	1.40546	1.40982	1.41300	1.41616	1.41869	1.42111
318.15	1.40413	1.40847	1.41164	1.41477	1.41727	1.41968

The data presented in this table were obtained taking into account the linear fitting of the raw experimental results for the refractive indices. Experimental data is presented as supporting information.
Note: the magnitude of the experimental differentiation between the two independent set of refractive indices data: ±0.00005.

Table 6
Experimental refractive indices at the sodium D-line, n_D, for the studied ionic liquids as a function of temperature at 0.1 MPa.

Ionic liquid	n_D (298.15 K)	$10^4 \cdot (dn_D/dT)/(K^{-1})$ [a]	n_D (298.15 K) literature
$[C_4C_1im][PF_6]$	1.40945	−2.66 ± 0.01	1.40890 [5] 1.40937 [6] 1.40950 [7] 1.40900 [8] 1.40925 [9] 1.40844 [18]
$[C_5C_1im][PF_6]$	1.41387	−2.70 ± 0.01	
$[C_6C_1im][PF_6]$	1.41708	−2.72 ± 0.02	1.41787 [6] 1.4169 [26] 1.41648 [18]
$[C_7C_1im][PF_6]$	1.42033	−2.78 ± 0.01	
$[C_8C_1im][PF_6]$	1.42293	−2.846 ± 0.005	1.4230 [8] 1.42302 [6] 1.42351 [18]
$[C_9C_1im][PF_6]$	1.42538	−2.85 ± 0.01	

[a] In the temperature interval, any value of n_D, at a specific temperature, T, can be estimated using the following equation: $n_D(T/K) = n_D\ (298.15\ K) + dn_D/dT \cdot (T/K - 298.15\ K)$.

$[PF_6]^-$ when compared with the $[NTf_2]^-$ that will be reflected on higher cohesive energies [49] of the $[C_{N-1}C_1im][PF_6]$ series. These findings are in agreement with molecular simulation results reported in the literature [50]. The authors found that for the $[C_{N-1}C_1im][PF_6]$, which possesses a smaller anion and higher charge density compared to the bistriflamide anion, the non-polar domains consist of islands in the continuous medium of polar network ($[C_3C_1im][PF_6]$ to $[C_4C_1im][PF_6]$), whereas starting from $[C_5C_1im][PF_6]$, a bi continuous segregated phase is established [50]. For the case of the bistriflamide anion, which is a bulkier anion, and possesses a lower charge density, the limit to start the nanostructuration is around $[C_6C_1im][NTf_2]$ as previously shown by us [1–4].

3.3. Refractive index

The measured refractive index data in the temperature range from 288 K to 318 K, are presented in Table 5. The graphic representation of the refractive indices as a function of the temperature for the studied ionic liquids is depicted in Fig. 6(I). Table 6 lists the refractive indices of all studied ionic liquids, at $T = 298.15$ K, the literature values, and the temperature derivative of the refractive index, dn_D/dT.

For all the ionic liquids, the refractive index values at 298.15 K obtained in this work are in good agreement with those previously reported in the literature (relative deviations are between 0.03% and −0.05%). As observed before [27], the temperature dependence of the refractive indices is less pronounced than the verified for the usual molecular solvents. For the studied ILs, a decrease in the refractive index of 0.00027 to 0.00029 per Kelvin along the alkyl side chain of the cation was found .

The plots of the refractive indices, at $T = 298.15$ K as a function of the total number of carbon atoms in the alkyl chains in the cation, for the $[C_{N-1}C_1im][PF_6]$ and their comparison with the $[C_{N-1}C_1im][NTf_2]$ [18], are shown in Fig. 6(II). The lower refractive indices of the $[PF_6]^-$ compared with $[NTf_2]^-$ the series arise from the lower polarizability of the $[PF_6]^-$ anion. A shift in the refractive indices trend along the alkyl side chain of the cation for the studied hexafluorophosphate based ILs, around $[C_7C_1im][PF_6]$, was found. Above this Critical Alkyl Length Size (CALS), $[C_7C_1im][PF_6]$, a decrease of the contribution per methylene group ($-CH_2-$) is observed. The shift in the refractive indices trend could be related with the nanostructuration/segregation that occurs after the CALS. After that, there is no significant change in the nearest cation–anion interaction potential and as consequence, the charge dispersion and the

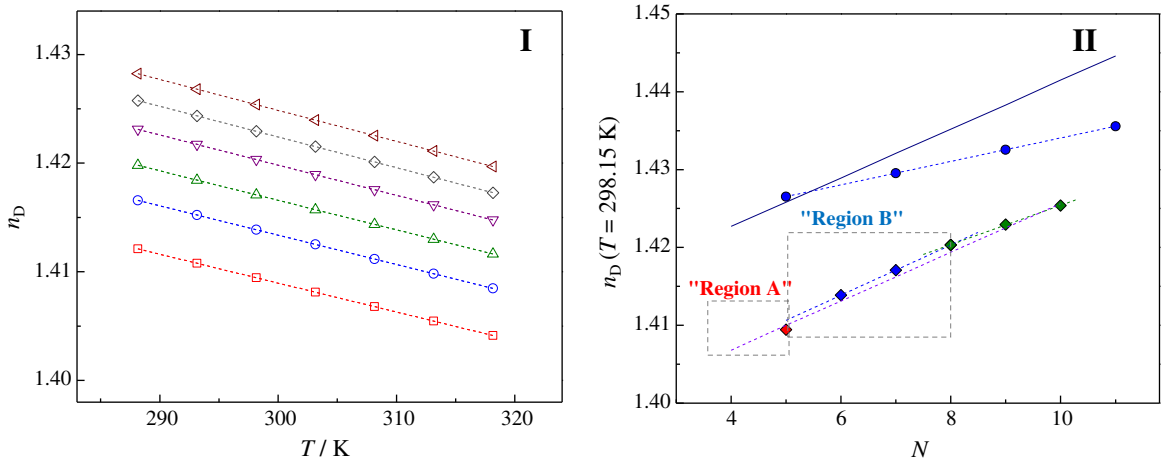

Fig. 6. (**I**) Graphical representation of the refractive indices as a function of temperature for $[C_{N-1}C_1im][PF_6]$ ionic liquid series. □ - $[C_4C_1im][PF_6]$; ○ - $[C_5C_1im][PF_6]$; △ - $[C_6C_1im][PF_6]$; ▽ - $[C_7C_1im][PF_6]$; ◇ - $[C_8C_1im][PF_6]$; ◁ - $[C_9C_1im][PF_6]$. (**II**) Refractive indices, n_D, at $T = 298.15$ K as function of the total number of carbon atoms in the alkyl side chains of the cation, N. ◆ - $[C_{N-1}C_1im][PF_6]$ (with $N = 5$ - 10) and ● - $[C_{N-1}C_1im][NTf_2]$ (with $N = 5, 7, 9, 11$) [18]. Gardas and Coutinho group contribution [44]: – – – - $[C_{N-1}C_1im][PF_6]$ ($N = 4$ - 10) and — - $[C_{N-1}C_1im][NTf_2]$ (with $N = 4$ - 11).

polarizability of the charged region remains almost unchanged, and with it the contribution to the refractive indices due to the polarizability.

4. Final remarks

The molecular interpretation of the thermophysical properties of the hexafluorophosphate based ionic liquids, and the comparison with the analogous NTf_2 series could only be done by taking into account the high degree of organization, the structural complexity, shape and size of the ions of the ionic liquids. For the same number of carbons in the alkyl chain, *N*, the hexafluorophosphate based ionic liquids present lower density and lower thermal expansion coefficients when compared with the $[C_{N-1}C_1im][NTf_2]$ IL series. The $[C_{N-1}C_1im][PF_6]$ ionic liquids present significantly higher viscosities than the bistriflamide based ILs, which are related with the higher energy barrier of the liquid to a shear stress. A trend shift along the alkyl side chain of the cation around $[C_7C_1im][PF_6]$, was found for the viscosities and refractive indices. The effect of the increase of the alkyl side chain on the interaction between the cation and anion is more pronounced in the ionic liquids with shorter alkyl side chain due to the high impact of the alkyl chain steric hindrance in the ions electrostatic interaction.

For ionic liquids with intermediate alkyl side chain lengths, there is a regular region where a decrease of the electrostatic interaction between the ions, is observed. From a critical alkyl length size, CALS (around $[C_7C_1im][PF_6]$) the nanostructuration into polar and non-polar regions begins and the effect of the decrease of the electrostatic interactions is partially compensated by the increase of the non-electrostatic interactions in the non-polar regions. After the CALS, the increase of the non-polar region leads to a new behavior where the $-CH_2-$ increment is similar to the one observed for the alkanes/alkane-derivatives where a smaller but progressive change of the overall polar network region is observed.

Acknowledgments

This work was supported by FCT, Lisbon, Portugal, and the European Social Fund through strategic projects Pest-C/QUI/UI0081/2011 awarded to CIQUP and Pest-C/CTM/LA0011/2011 to CICECO. M.A.A. Rocha and A.I.M.C.L. Ferreira acknowledge the financial support from FCT for the award of research grants with references, SFRH/BD/60513/2009 and SFRH/BPD/84891/2012 respectively.

Appendix A. Supplementary data

Experimental refractive indices at the sodium D-line, nD, at 0.1 MPa, for the studied ionic liquids as a function of temperature. Supplementary data to this article can be found online at http://dx.doi.org/10.1016/j.molliq.2013.09.031.

References

[1] M.A.A. Rocha, C.F.R.A.C. Lima, L.R. Gomes, B. Schröder, J.A.P. Coutinho, I.M. Marrucho, J.M.S.S. Esperança, L.P.N. Rebelo, K. Shimizu, J.N. Canongia Lopes, L.M.N.B.F. Santos, J. Phys. Chem. B 115 (2011) 10919.
[2] M.A.A. Rocha, M. Bastos, J.A.P. Coutinho, L.M.N.B.F. Santos, J. Chem. Thermodyn. 53 (2012) 140.
[3] M.A.A. Rocha, J.A.P. Coutinho, L.M.N.B.F. Santos, J. Phys. Chem. B 116 (2012) 10922.
[4] M.A.A. Rocha, C.M.S.S. Neves, M.G. Freire, O. Russina, A. Triolo, J.A.P. Coutinho, L.M.N.B.F. Santos, J. Phys. Chem. B (2013), http://dx.doi.org/10.1021/jp406374a.
[5] A. Kumar, J. Solut. Chem. 37 (2008) 203–214.
[6] A.B. Pereiro, A. Rodríguez, J. Chem. Eng. Data 52 (2007) 600–608.
[7] M.T. Zafarani-Moattar, R. Majdan-Cegincara, J. Chem. Eng. Data 52 (2007) 2359–2364.
[8] J.G. Huddleston, A.E. Visser, M. Reichert, H.D. Willauer, G.A. Broker, R.D. Rogers, Green Chem. 3 (2001) 156–164.
[9] M. Bendová, Z. Wagner, J. Chem. Eng. Data 51 (2006) 2126–2131.
[10] G.J. Kabo, A.V. Blokhin, Y.U. Paulechka, A.G. Kabo, M.P. Shymanovich, J.W. Magee, J. Chem. Eng. Data 49 (2004) 453–461.
[11] C.P. Fredlake, J.M. Crosthwaite, D.G. Hert, S.N.V.K. Aki, J.F. Brennecke, J. Chem. Eng. Data 49 (2004) 954–964.
[12] J. Jacquemin, P. Husson, A.A.H. Padua, V. Majer, Green Chem. 8 (2006) 172–180.
[13] D. Tomida, A. Kumagai, K. Qiao, C. Yokoyama, Int. J. Thermophys. 27 (2006) 39–47.
[14] Y. Geng, S. Chen, T. Wang, D. Yu, C. Peng, H. Liu, Y. Hu, J. Mol. Liq. 143 (2008) 100–108.
[15] D. Tomida, A. Kumagai, S. Kenmochi, K. Qiao, C. Yokoyama, J. Chem. Eng. Data 52 (2007) 577–579.
[16] R. Taguchi, H. Machida, Y. Sato, R.L. Smith Jr., J. Chem. Eng. Data 54 (2009) 22–27.
[17] J. Troncoso, C.A. Cerdeiriña, Y.A. Sanmamed, L. Romaní, L.P.N. Rebelo, J. Chem. Eng. Data 51 (2006) 1856.
[18] M. Tariq, P.A.S. Forte, M.F.C. Gomes, J.N.C. Lopes, L.P.N. Rebelo, J. Chem. Thermodyn. 41 (2009) 790–798.
[19] A. Ahosseini, A.M. Scurto, Int. J. Thermophys. 29 (2008) 1222–1243.
[20] A.B. Pereiro, J.L. Legido, A. Rodríguez, J. Chem. Thermodyn. 39 (2007) 1168–1175.
[21] W. Fan, Q. Zhou, J. Sun, S. Zhang, J. Chem. Eng. Data 54 (2009) 2307–2311.
[22] K.R. Harris, M. Kanakubo, L.A. Woolf, J. Chem. Eng. Data 51 (2006) 1161–1167.
[23] K.R. Harris, M. Kanakubo, L.A. Woolf, J. Chem. Eng. Data 52 (2007) 1080–1085.
[24] L.C. Branco, J.N. Rosa, J.J.M. Ramos, C.A.M. Afonso, Chem. Eur. J. 8 (2002) 3671–3677.
[25] H. Tokuda, S. Tsuzuki, Md.A.B.H. Susan, K. Hayamizu, M. Watanabe, J. Phys. Chem. B 110 (2006) 19593–19600.
[26] A. Muhammad, M.I. Abdul Mutalib, C.D. Wilfred, T. Murugesan, A. Shafeeq, J. Chem. Thermodyn. 40 (2008) 1433–1438.
[27] M.G. Freire, A.R.R. Teles, M.A.A. Rocha, B. Schröder, C.M.S.S. Neves, P.J. Carvalho, D.V. Evtuguin, L.M.N.B.F. Santos, J.A.P. Coutinho, J. Chem. Eng. Data 56 (2011) 4813–4822.
[28] Y. Yu, A.N. Soriano, M. Li, Thermochim. Acta 42 (2009) 482.
[29] John D. Holbrey, W. Matthew Reichert, Ramana G. Reddy, Robin D. Rogers, ACS Symp. Ser. 856 (2003) 121–133.
[30] C.A. Nieto de Castro, M.J.V. Lourenço, A.P.C. Ribeiro, E. Langa, S.I.C. Vieira, J. Chem. Eng. Data 55 (2010) 653–661.
[31] A.B. Pereiro, J.L. Legido, A. Rodríguez, J. Chem. Thermodyn. 38 (2006) 651–661.
[32] P.J. Carvalho, T. Regueira, L.M.N.B.F. Santos, J. Fernandez, J.A.P. Coutinho, J. Chem. Eng. Data 55 (2010) 645–652.
[33] R.L. Gardas, M.G. Freire, P.J. Carvalho, I.M. Marrucho, I.M.A. Fonseca, A.G.M. Ferreira, J.A.P. Coutinho, J. Chem. Eng. Data 52 (2007) 80–88.
[34] M.E. Wieser, M. Berglund, Pure Appl. Chem. 81 (2009) 2131–2156.
[35] J. Suurkuusk, I. Wadsö, J. Chem. Thermodyn. 6 (1974) 667–679.
[36] J. Konicek, J. Suurkuusk, I. Wadsö, Chem. Scr. 1 (1971) 217–220.
[37] L.M.N.B.F. Santos, M.A.A. Rocha, A.S.M.C. Rodrigues, V. Štejfa, M. Fulem, M. Bastos, J. Chem. Thermodyn. 43 (2011) 1818–1823.
[38] C.E.S. Bernardes, L.M.N.B.F. Santos, M.E. Minas da Piedade, Meas. Sci. Technol. 17 (2006) 1405–1408.
[39] R. Sabbah, A. Xu-wu, J.S. Chickos, M.L.P. Leitão, M.V. Roux, L.A. Torres, Thermochim. Acta 331 (1999) 93–204.
[40] R.D. Chirico, V. Diky, J.W. Magee, M. Frenkel, K.N. Marsh, Pure Appl. Chem. 81 (2009) 791–828.
[41] M.E. Wieser, T.B. Coplen, Pure Appl. Chem. 83 (2011) 359–396.
[42] M. Tariq, A.P. Serro, J.L. Mata, B. Saramago, J.M.S.S. Esperança, J.N. Canongia Lopes, L.P.N. Rebelo, Fluid Phase Equilib. 294 (2010) 131–138.
[43] C.M.S.S. Neves, M.L.S. Batista, A.F.M. Cláudio, L.M.N.B.F. Santos, I.M. Marrucho, M.G. Freire, J.A.P. Coutinho, J. Chem. Eng. Data 55 (2010) 5065–5073.
[44] R.L. Gardas, J.A.P. Coutinho, AIChE J. 55 (2009) 1274–1290.
[45] David R. Lide, CRC Handbook of Chemistry and Physics, 84th edition Taylor & Francis, 2003.
[46] K.R. Seddon, A. Stark, M. Torres, J. Pure Appl. Chem. 72 (2000) 2275–2287.
[47] K.R. Seddon, A. Stark, M. Torres, , Chapter 4 ACS Symp. Ser. (2002) 34–49.
[48] D.S. Viswanath, T.K. Ghosh, D.H.L. Prasad, N.V.K. Dutt, K.Y. Rani, Viscosity of Liquids: Theory, Estimation, Experiment, and Data, Springer, Netherlands, 2007.
[49] H. Vogel, Phys. Z. 22 (1921) 645.
[50] G.S. Fulcher, J. Am. Ceram. Soc. 8 (1925) 339.
[51] G. Tammann, W. Hesse, Z. Anorg. Allg. Chem. 156 (1926) 245.
[52] M. Tariq, P.J. Carvalho, J.A.P. Coutinho, I.M. Marrucho, J.N.C. Lopes, L.P.N. Rebelo, Fluid Phase Equilib. 301 (2011) 22–32.
[53] J.N.A. Canongia Lopes, A.A.H. Pádua, J. Phys. Chem. B 110 (2006) 3330–3335.